Title
Site Characterization for Selected Liquefaction Case History Sites from February 6, 2023, Türkiye-Kahramanmaras Earthquakes

Journal
GeoCongress 2026

Authors
Sahin, Arda
Moss, Robb E.S.
Cetin, Kemal O.
et al.

Publication Date
2026-03-01

Data Availability
The data associated with this publication are available at: https://doi.org/10.17603/ds2-71fz-gy07

Peer reviewed

Site Characterization for Selected Liquefaction Case History Sites from February 6, 2023, Türkiye-Kahramanmaras Earthquakes

Arda Sahin, Ph.D. Candidate, S.M.ASCE[1], Robb Eric S. Moss, Ph.D., F.ASCE[2], Kemal Onder Cetin, Ph.D., M.ASCE[3], Scott J. Brandenberg, Ph.D., M.ASCE[4], Jonathan P. Stewart, Ph.D., F.ASCE[5], and Tristan E. Buckreis, Ph.D., M. ASCE[6]

[1]University of California, Los Angeles, Los Angeles, CA 90095, USA,
Email: arda120222@g.ucla.edu
[2]California Polytechnic State University, San Luis Obispo, CA 93407, USA,
Email: rmoss@calpoly.edu
[3]Middle East Technical University, 06800, Türkiye,
Email: ocetin@metu.edu.tr
[4]University of California, Los Angeles, Los Angeles, CA 90095, USA,
Email: sjbrandenberg@g.ucla.edu
[5]University of California, Los Angeles, Los Angeles, CA 90095, USA,
Email: jstewart@seas.ucla.edu
[6]University of California, Los Angeles, Los Angeles, CA 90095, USA,
Email: tristanbuckreis@ucla.edu

ABSTRACT

For a series of sites with post-event observations from GEER Association reconnaissance activities in the regions affected by two large earthquakes in Türkiye on February 6, 2023, we present the results of targeted site investigations. Four investigated sites are near critical ground motion accelerometer/seismometer sites where ground failure from liquefaction was either observed to have occurred or was observed to have not occurred but might reasonably have been anticipated based on surface geology. Two additional sites located in Hatay–Antakya–Demirköprü have been investigated. One on a point bar of the Orontes River experienced liquefaction manifestations in the form of lateral spreading and soil ejecta while the second in a cut bank experienced minor to no ground failure. The investigations performed include borings with standard penetration testing, cone penetration testing that includes downhole shear wave travel time measurements, surface wave dispersion curves, and laboratory testing of samples recovered from the field. The main point of this paper is to present the data that have been assembled using standard templates and added to the Next Generation Liquefaction database, which will support future modeling efforts.

Measurements from sites near ground motion stations are used to correct the estimated V_{S30} values in the Next Generation Attenuation-West3 database. The uncertainty associated with these measurements is quantified. The resulting V_{S30} values are used to derive non-ergodic site responses at the recording sites. Case history sites located in Hatay–Antakya–Demirköprü are examined using two legacy models and the recent Next Generation Liquefaction (NGL) triggering–manifestation model. One of the sites experienced surface manifestation, which was correctly predicted by each of the models (true positive predictions). Another site did not have manifestation, which was incorrectly predicted by legacy models that use a critical layer framework (false positive prediction) but was correctly predicted by the NGL model (true negative).

INTRODUCTION

On February 6, 2023, two earthquakes struck the southeastern part of Türkiye, nine hours apart: the Pazarcık Earthquake (**M**7.81) and the Ekinozu Earthquake (**M**7.74). The Pazarcık Earthquake was followed by an aftershock of **M**6.81, named the Nurdağı Earthquake. Moreover, thirteen days later, another earthquake was recorded in the southern Hatay region with a magnitude of **M**6.37. Many researchers, including members of the GEER Association, conducted extensive reconnaissance activities (Cetin et al., 2023; and Moug et al., 2023) to document perishable field data following the earthquakes. Observations included many examples of ground failure across a large area, which in many cases damaged infrastructure.

We present preliminary results of an NSF-funded Rapid research study jointly conducted by UCLA, Cal Poly, METU, and Cal State Fullerton researchers. The study included site investigations such as seismic Cone Penetration Tests (sCPT), borings with Standard Penetration Tests (SPT), refraction tests, and laboratory tests on collected samples, along with fault trenching operations. The work presented here is one among several post-event investigations, which are summarized in Table 1. Subsequent sections of this paper summarize the collected data, assess current liquefaction manifestation and triggering models relative to the data for the selected sites, and highlight their importance and implications. The data produced in this investigation is being prepared for publication through DesignSafe-CI.

Table 1. Studies pertaining to ground motion recordings or site characterization at ground failure sites following the 2023 Türkiye Earthquakes

Publication Type	Classification	Reference
Journal Paper	Ground motions	Asadi et al. (2024), Cetin et al. (2024d), Elsaid and Cetin (2024), Buckreis et al. (2024)
	Dams	Cetin et al. (2024a, 2025), Lashgari & Moss (2024)
	Golbasi region-specific	Cetin et al. (2024b), Karakas et al. (2024)
	Hatay region-specific	Bassal et al. (2024), Bol et al. (2024), Cakir and Cetin (2024), Cetin et al. (2024c), Ocak and Cetin (2024), Ozener et al (2024), Ozkaynak and Cetin (2024), Sahin and Cetin (2024), Moug et al. (2024c)
Dataset	Iskenderun, Hatay region-specific	Macedo et al. (2025a), Moug et al. (2024b)
	Golbasi region-specific	Macedo et al. (2025b), Moug et al. (2024a)

INVESTIGATION LOCATIONS

Figure 1 shows the locations of the six investigated sites – four at ground motion stations (Sites 3-6) and two liquefaction sites (Sites 1-2). In this figure, the finite fault models selected by Buckreis et al. (2024) for the Pazarcık Earthquake (red lines) and Ekinozu Earthquake (yellow boxes) are shown. Site 7 is the location of fault trenching operations conducted as part of this study but not discussed in this paper.

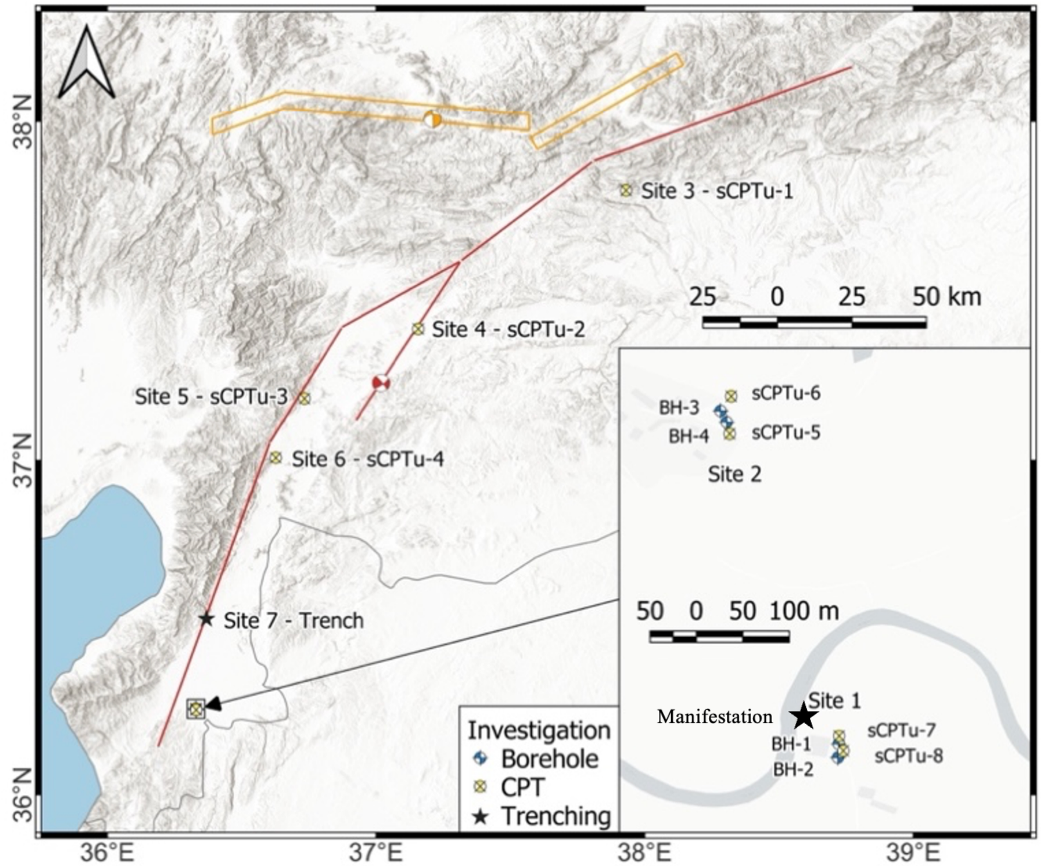

Figure 1. Map showing the locations of investigated sites with surface projections of selected finite fault models (Buckreis et al. 2024) and borehole / CPT identification numbers

Each of the strong motion sites considered in this research was visited following the earthquake sequence and no evidence of ground failure was observed. The investigated ground motion station sites produced crucial near-fault (i.e., $R_{rup} < 5$ km), large-magnitude recordings that have been implemented in the global Ground Motion Database (Buckreis et al. 2025a), which is being used in the database for the ongoing Next Generation Attenuation-West3 (NGA-West3) project (Buckreis et al. 2025b,c). The ability of engineers and seismologists to utilize the recordings in engineering applications is significantly enhanced when site characterization data is available. Figure 2 shows the locations of the data points associated with these four sites within the NGA-West2 database. Blue points indicate all ground motion stations with recordings, while red points represent the investigated ground motion stations.

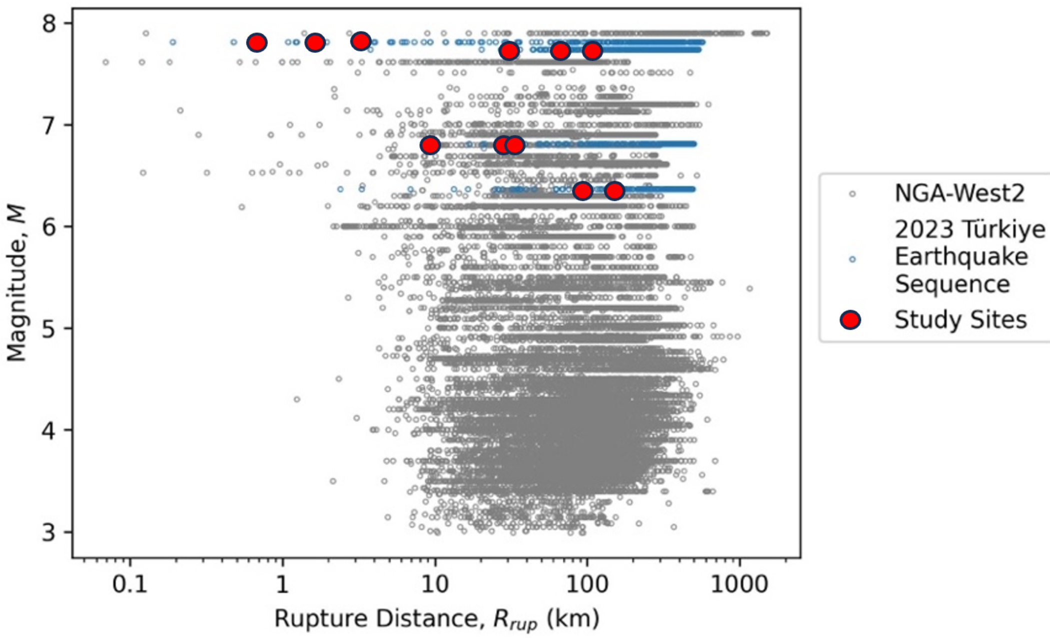

Figure 2. Recordings in the NGA-West2 database with added data highlighted

The results of the reconnaissance of the bridge case history sites in Hatay–Antakya–Demirköprü are reported in the GEER report (Cetin et al., 2023). As discussed in that report and by Ocak and Cetin (2024), the existing bridge structure was affected by lateral spreading and excessive settlement, which led to the rotational failure of the south abutment. While that site was unavailable for site characterization work, nearby reconnaissance observations are available at Sites 1 and 2, located 2 to 3 km away from the bridge site. At Site 1, lateral spreading and soil ejecta were observed in a point bar, while at Site 2, minor to no ground failure was noted in a cut bank. The locations of these observations are shown in Figure 1.

SITE CHARACTERIZATION FOR GROUND MOTION STATIONS

The principal objective of site characterization at ground motion stations was shear wave velocity (V_S) profiles from which time-averaged shear wave velocity for the upper 30 meters (V_{S30}) could be computed. Shear wave velocity profiles were measured using downhole tests in the form of sCPTs. However, at two of the sites, the CPT probe could not be advanced due to the gravelly nature of the soil; therefore, refraction methods were implemented instead. The locations of the sites, along with the test types used, are summarized in Table 2. Figure 3 shows example results for sCPTu-1 along with the refraction results for sites 4 and 6.

Table 2. Studies on seismic ground failures after 2023 Turkiye Earthquakes

Site #	Location	Station Code	Latitude	Longitude	Test Type
Site 3	Gaziantep - Islahiye	TK-2718	37.0078	36.6266	sCPTu
Site 4	Adiyaman - Tut	TK-0213	37.7967	37.9296	Refraction
Site 5	Gaziantep - Nurdagi	TK-2712	37.1840	36.7328	sCPTu
Site 6	K.Maras - Pazarcik	TK-4615	37.3868	37.1380	Refraction

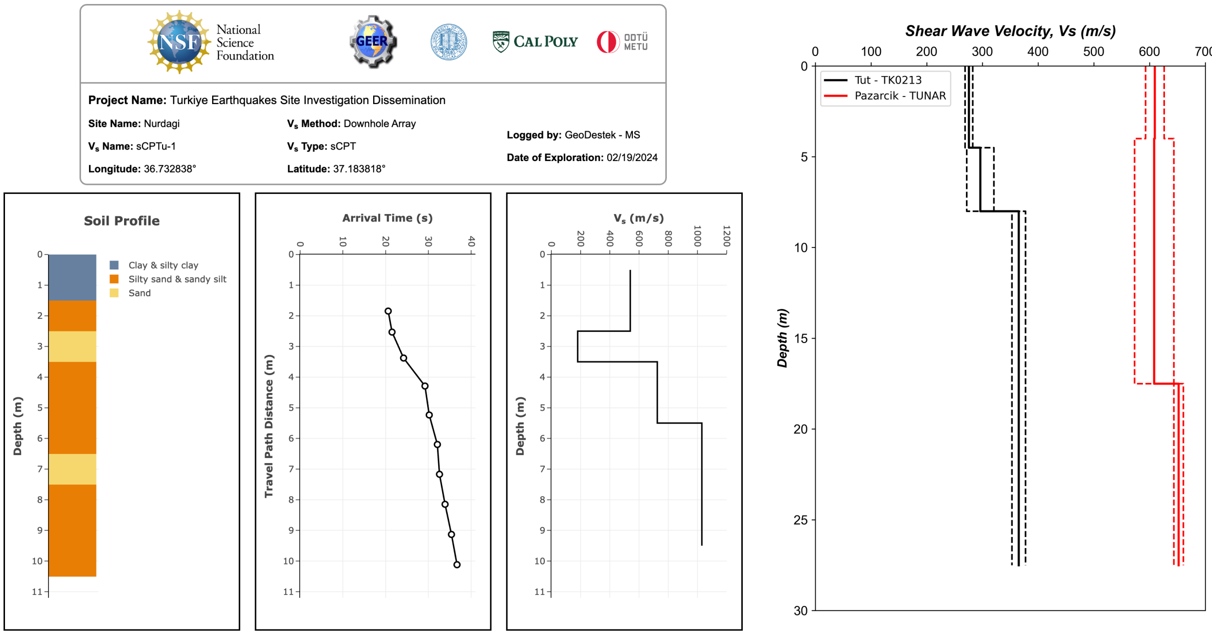

a) sCPTu-1 from Gaziantep- Nurdagi results **b) Refraction results**

Figure 3. sCPTu and refraction results

In a study of ground motion attributes following the 2023 Türkiye earthquakes, Buckreis et al. (2024) estimated V_{S30} values for the four sites in Table 2 using the method by Zhou (2023), which relies on the topographical slope from a digital elevation model. An exception is the Tut site where measurements were available from the Disaster and Emergency Management Authority (AFAD). Due to questions regarding the reliability of the AFAD testing, we retested one site (Tut). Table 3 provides values of V_{S30} reported by Buckreis et al. (2024).

Table 3. V_{S30} comparisons for the ground motion stations (Bea24 = Buckreis et al. 2024)

Site #	**Location**	**Station**	***Test Type***	$V_{SZ,measured}$ **(m/s)**	$V_{S30,projected}$ **(m/s)**	$V_{S30,est,Bea\ 24}$ **(m/s)**
Site 3	Gaziantep – Islahiye	TK-2718	sCPTu	360 ± 100	410 ± 140	528 m/s - Proxy
Site 4	Adiyaman – Tut	TK-0213	Refraction	365 ± 15	345 ± 25	684 m/s - Proxy
Site 5	Gaziantep – Nurdagi	TK-2712	sCPTu	900 ± 100	850 ± 300	482 m/s - Proxy
Site 6	K.Maras – Pazarcik	TK-4615	Refraction	652 ± 10	630 ± 40	484 m/s - AFAD

sCPT profiles reached depths of up to 9 m at Sites 3 and 5. The refraction tests performed at Sites 4 and 6 produced V_S profiles that extend to depths of up to 27 m. Time-averaged velocities to the profile depth (denoted V_{SZ}) are given in Table 3. Projections are needed to estimate V_{S30} values, which was done using the model by Dai et al. (2013) with global coefficients from Kwak et al. (2017) (no region-specific coefficients are available for Türkiye). As shown in Table 3, uncertainties in V_{SZ} values were estimated based on arrival times and 2D profile produced by the refraction measurements. V_{S30} uncertainties reported in Table 3 also include uncertainty from the depth projections.

Using the newly measured V_{S30} values, ground-motion residuals (natural log difference of ground motion intensity measure from data and model) were computed using the Boore et al. (2014) ground motion model. Partitioning of ground-motion residuals using mixed-effects analysis provided within-event residuals at each station. Figure 4 shows statistics (mean ± one standard deviation) of within-event residuals for each station, which provide an estimate of site response that can reveal features such as resonant peaks (e.g., peak at TK-0213 at about 0.5 sec). Alternate values that reflect the impact of V_{S30} uncertainties are shown, which are generally small.

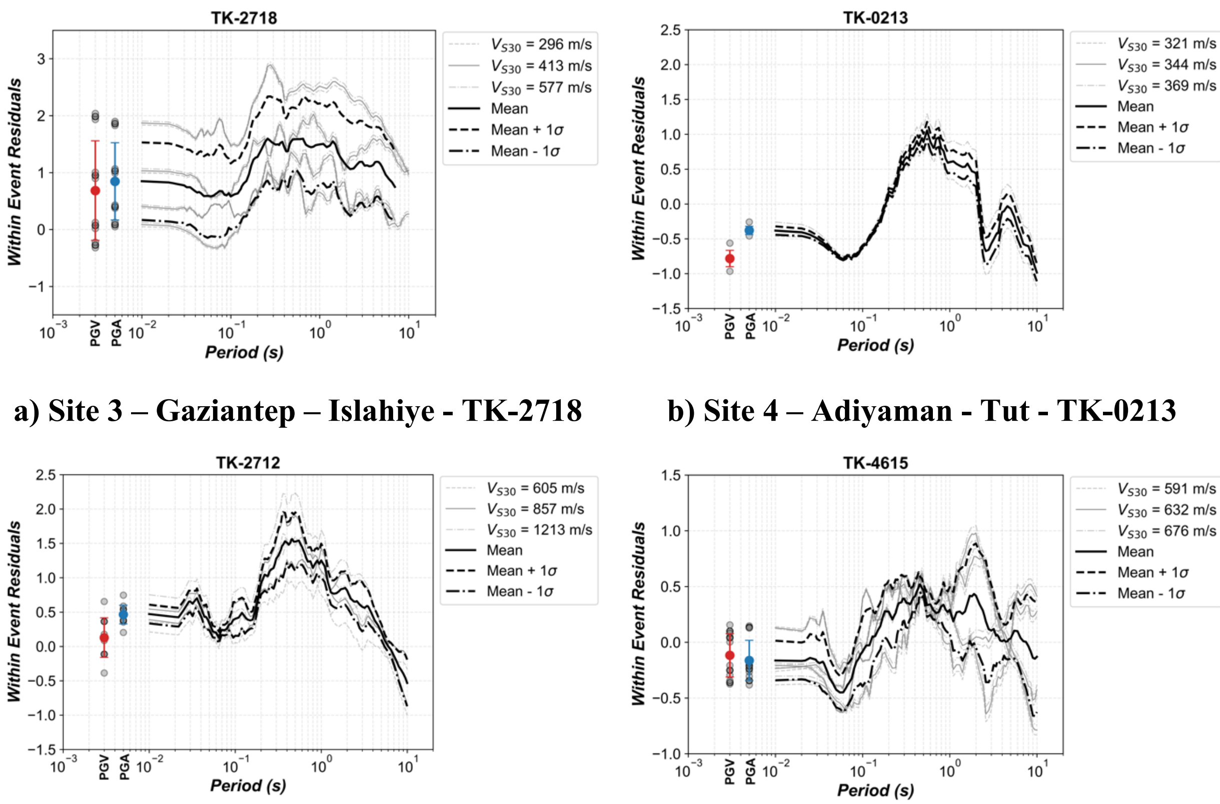

a) Site 3 – Gaziantep – Islahiye - TK-2718 **b) Site 4 – Adiyaman - Tut - TK-0213**

c) Site 5 – Gaziantep – Nurdagi -TK-2712 **d) Site 6 – K.Maras – Pazarcik - TK-4615**

Figure 4. Within event ground-motion residuals for recordings at Sites 3-6

APPLICATION OF LIQUEFACTION MODELS

Sites 1 and 2 in the Hatay–Antakya–Demirköprü region were investigated (Figure 1). Site 1 was affected by the 2023 Türkiye earthquake sequence, including manifestations such as lateral spreading, and soil ejecta within an Orontes River Point Bar. On the other hand, Site 2 experienced minor affects to no manifestation in a cut bank area. Between the two sites, four boreholes and four sCPTs were performed. Laboratory index tests on collected soil specimens were conducted for soil classification purposes (fines content and plasticity).

We use all sCPTs to assess both triggering and manifestation using two legacy CPT-based models—Boulanger and Idriss (2016) and Moss et al. (2006)—as well as the recent NGL triggering and manifestation model (Ulmer et al., 2024). The fundamental difference between the legacy and NGL models is that while the legacy models assess triggering and manifestation jointly (assuming perfect correlation between the two) and utilize only a critical layer from the soil profile, the NGL model separates these phenomena and consider the entire soil profile.

Figure 5 shows co-located BH-1 and sCPTu-7 logs as a representative result. The CPT results revealed features in both tip and friction resistances—defined as "spikes" at roughly one-meter intervals—which were likely caused by stress relief as new rods were added. These artifacts were removed using the "spike" filter described in the RocScience (2021) Theory Manual. The corrected version is shown with the red lines in Figure 5.

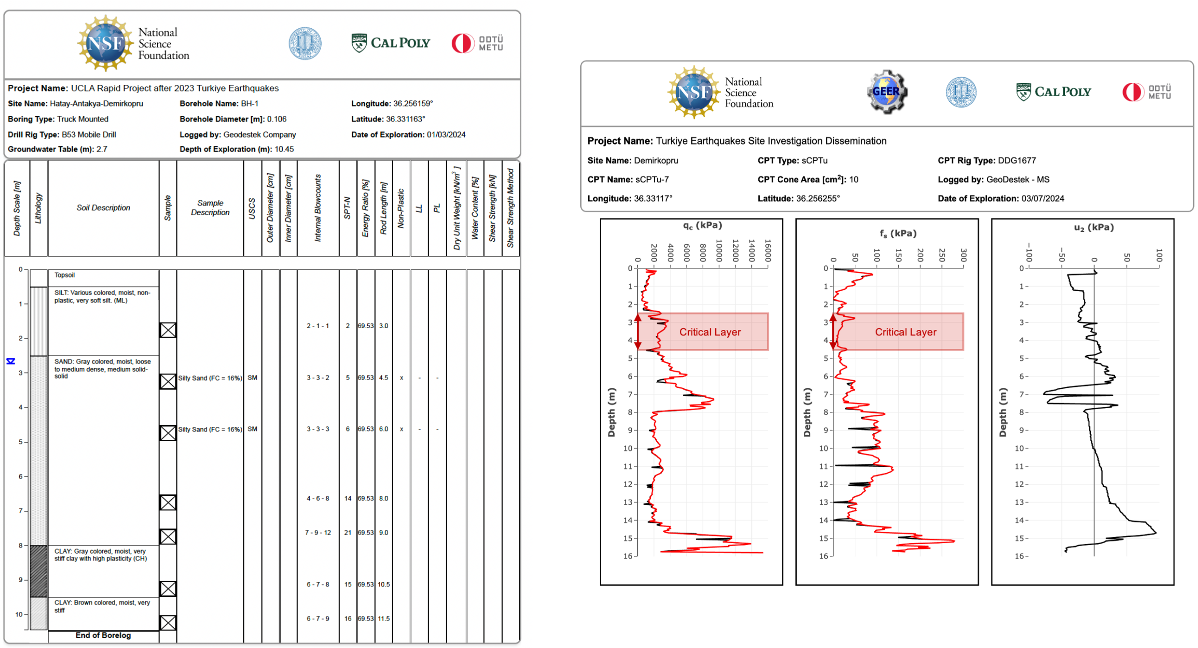

a) BH-1 results **b) sCPTu-7 results**

Figure 5. Representative soil stratigraphy. Critical layer used with legacy models shown.

For the liquefaction triggering and manifestation assessments, the earthquake magnitude was selected as **M**7.81 and the peak ground acceleration (*PGA*) as 0.46g, based on Pretell et al. (2024) for the Pazarcık event, to be used as input parameters for the models. Critical layers were selected using analyst judgement and corresponding penetration resistances and cyclic stress ratios (CSRs) is shown in Figure 6.

No critical layer was selected for sCPTu-5 because the profile mostly consists of a high soil behavior type index, I_c (i.e., $I_c > 2.6$) layer between 0.5 – 8.0 m, which is also evident in BH-4. In the judgment of legacy model developers that are also authors of this paper, the materials at that site are too plastic to be susceptible. Two different points shown as sCPTu-6a and sCPTu-6b are selected for sCPTu-6. These two layers are both viable selections as the critical layer based on interpretations by different members of the author team. The upper layer is located between 3.5 – 4.5 m with an average $I_c = 2.1$ (i.e., sandy silt) with lower tip resistance, whereas a deeper layer from 4.5 – 5.0 m has lower I_c however and higher tip resistance.

Both models indicate a high probability of liquefaction for both Sites 1 and 2, which can be interpreted as consistent with the field observations of liquefaction manifestation for Site 1 but inconsistent with Site 2 (recall that sCPTu-5 is not assessed because it lacks a susceptible layer).

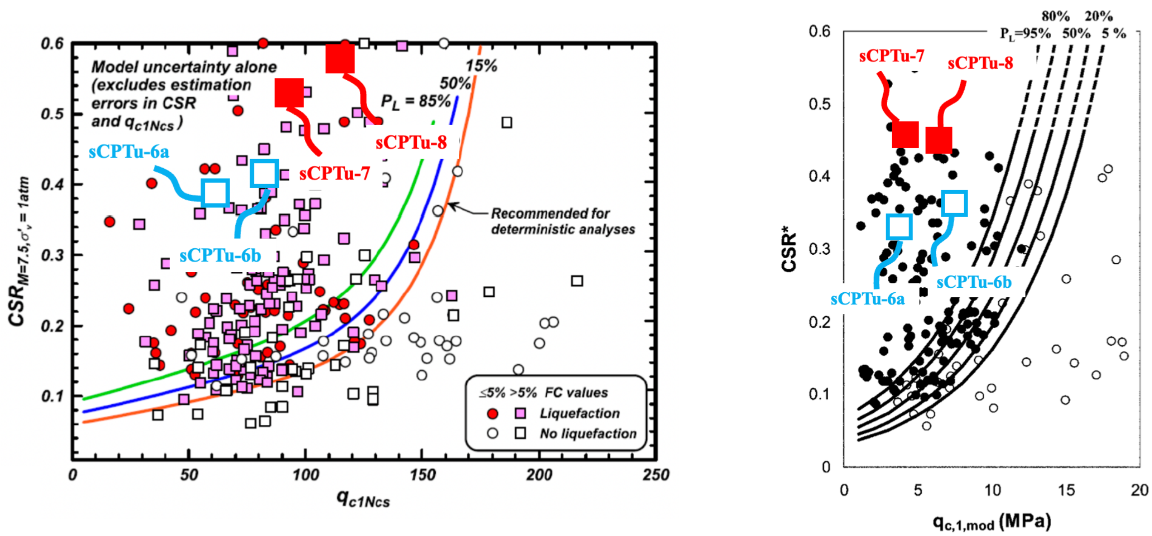

a) Boulanger and Idriss (2016)

b) Moss et al. (2006)

Figure 6. Case history overlays on legacy models for CPTs at Sites 1 and 2, **M**7.81 Pazarcık event

The profile analysis using the NGL triggering, and manifestation model were performed using ngl_tools (Hudson et al., 2024). The graphical profile-based solution of the model is presented in Figure 7 for sCPTu-7, which is at a location where manifestation was observed in the form of ejecta and lateral spreading and indicates a profile manifestation probability of 88.7%. Fragility curves generated by the ngl_tools based on different magnitude and *PGA* values are shown in Figure 8 for sCPTu-7. It should be noted that fragility curves do not exceed 89% due to susceptibility criteria in the model.

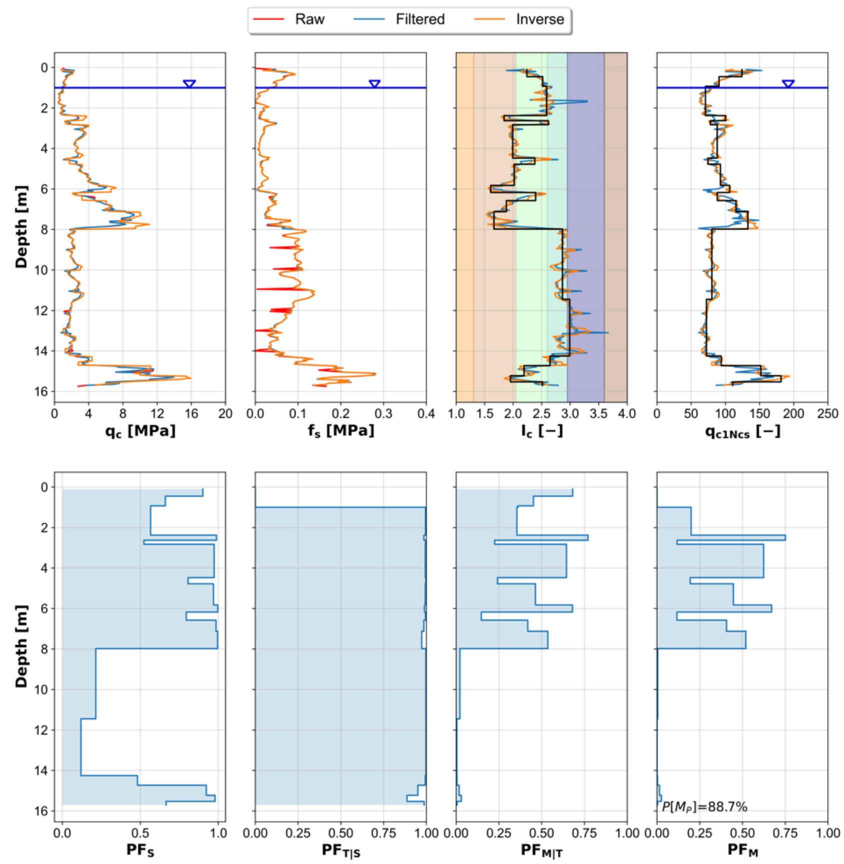

Figure 7. Ulmer et al. (2024) triggering-manifestation model applied to sCPTu-7 for a selected PGA = 0.46g and **M**=7.81. PF_S, $PF_{T|S}$, $PF_{M|T}$, and PF_M are probability factors for susceptibility, triggering given susceptibility, manifestation given triggering, and manifestation, respectively.

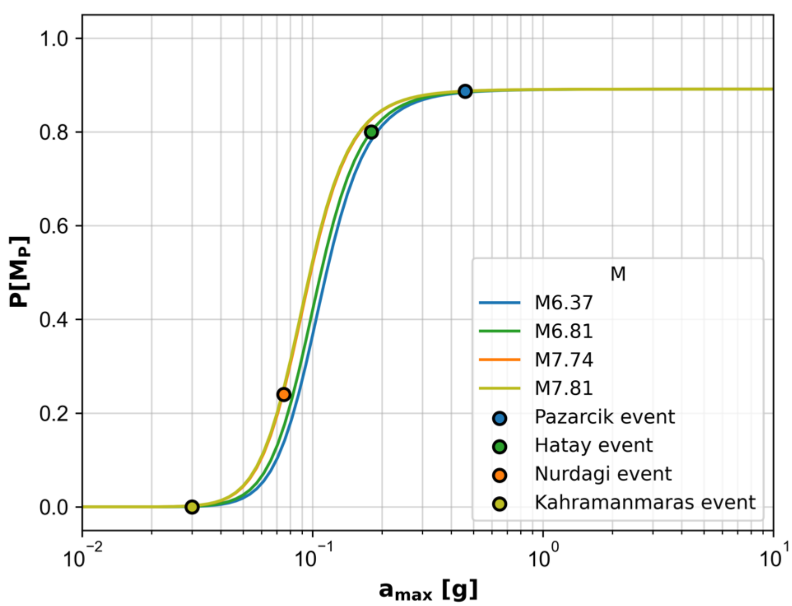

Figure 8. Ulmer et al. (2024) triggering-manifestation model fragility curves applied to sCPTu-7

Table 4 summarizes results for probability of manifestation (NGL model) and conditional probability of triggering given susceptibility (legacy models) for all sCPTs at Sites 1 and 2 for the Pazarcık event. The legacy models yield high conditional probabilities of triggering for both of the sites. The NGL model predicts a probability of manifestation greater than 50% for all sCPTs except sCPTu-5, which is consistent with the observations. The sCPTu-5 log is amenable to analysis in the NGL framework because susceptibility analysis is embedded within the approach. The low manifestation probability is mainly a consequence of limited susceptibility associated with the high- I_c (i.e., $I_c > 2.5$) soil layer between 0.5 and 8.0 m depth.

In the case of sCPTu-6, two different critical layers have been investigated for the legacy models. Both layers yield high probabilities from both legacy models. The NGL profile manifestations are lower (57%) than from the legacy models. These differences between legacy and NGL models may be due to triggering occurring at this location without manifestation. This could occur because the critical layer is relatively thin (i.e., ~0.5 to 1 m) and is located between high-I_c soil layers. As a result, this case history is considered valuable for future modeling efforts.

Table 4. Probability of manifestation and triggering results for Ulmer et al. (2024), Boulanger and Idriss (2016) and Moss et al. (2006) models for Pazarcık event

Site #	Manifested?	sCPTu #	Probability of Manifestation, P[M_P]	Probability of Triggering conditioned on susceptibility, $P_{L\|S}$	
			Ulmer et al. (2024)	Boulanger and Idriss (2016)	Moss et al. (2006)
Site 1	Yes	sCPTu-7	88.7%	~100%	~100%
		sCPTu-8	74.1%	~100%	~100%
Site 2	No	sCPTu-5	18.0%	Not Susceptible	
		sCPTu-6a	57.3%	~100%	~100%
		sCPTu-6b		~100%	~100%

CONCLUSION

After the 2023 Türkiye earthquakes, extensive ground failure was observed that was documented in reconnaissance reports including Cetin et al. (2023). To develop those observations into usable case histories, site investigation studies have been carried out in this study and several other studies summarized in Table 1. The aims of the work described here were to: (*i*) geotechnically characterize liquefaction-affected sites to develop usable case histories, and (*ii*) develop V_S profiles for four near-fault sites to facilitate site response and ground motion modeling. Values of V_{S30} are provided here that update prior estimates from Buckreis et al. (2024) and are being implemented in the NGA-West3 database.

Geotechnical site characterization was performed for a liquefaction case history site (Site 1), where extensive surface manifestations were observed in the form of lateral spreading and soil ejecta, along with a nearby site (Site 2) where minor to no ground failure was observed. For validation purposes, two legacy models and the NGL triggering–manifestation model were used to estimate the probability of liquefaction triggering and manifestation for the Pazarcık event. The model estimations were generally consistent with the observations, except for sCPTu-6, where minor to no ground failure was observed. The absence of manifestation at this location can be attributed to the presence of a thin liquefiable layer (i.e., ~1 m) located between high-I_c soil layers, as reflected in the NGL model predictions. These case histories are being incorporated into the NGL database (Ulmer et al., 2023) and are considered valuable for future modeling efforts.

REFERENCES

Asadi, A., Sanon, C., Cakir, E., Zhan, W., Shirzadi, H., Baise, L. G., Cetin, K. O., & Moaveni, B. (2024). Geospatial liquefaction modeling of the 2023 Türkiye earthquake sequence by an ensemble of global, continental, regional, and event-specific models. *Seismological Research Letters*, 95(2A), 697–719. https://doi.org/10.1785/0220230287

Bassal, P., Papageorgiou, E., Moug, D. M., Bray, J. D., Cetin, K. O., Şahin, A., Kubatko, E. J., Nepal, S., Toth, C., Kendır, S. B., & Bikçe, M. (2024). Liquefaction ground deformations and cascading coastal flood hazard in the 2023 Kahramanmaraş earthquake sequence. *Earthquake Spectra*, 40(3), 1845–1869. https://doi.org/10.1177/87552930241247830

Bol, E., Özocak, A., Sert, S., Çetin, K. Ö., Arslan, E., Kocaman, K., & Ayhan, B. U. (2024). Evaluation of soil liquefaction in the city of Hatay triggered after the February 6, 2023 Kahramanmaraş-Türkiye earthquake sequence. *Engineering Geology*, 339, 107648. https://doi.org/10.1016/j.enggeo.2024.107648

Boulanger, R. W., & Idriss, I. M. (2016). CPT-Based Liquefaction Triggering Procedure. *Journal of Geotechnical and Geoenvironmental Engineering*, 142(2). https://doi.org/10.1061/(asce)gt.1943-5606.0001388

Boore, DM, JP Stewart, E Seyhan, and GM Atkinson (2014). NGA-West2 equations for predicting PGA, PGV, and 5%-damped PSA for shallow crustal earthquakes, Earthquake Spectra, 30(3), 1057-1085. https://doi.org/10.1193/070113EQS184M

Buckreis, T. E., Pretell, R., Sandikkaya, M. A., Kale, Ö., Askan, A., Brandenberg, S. J., & Stewart, J. P. (2024). Engineering attributes of ground motions from February 2023 Türkiye earthquake sequence. *Earthquake Spectra*, 40(4), 2268–2284. https://doi.org/10.1177/87552930241259024

Buckreis, T. E., Shams, R., Mohammed, S., Li, M., Kishida, T., Lanzano, G., Luzi, L., Zimmaro, P., Huang, J.-Y., Bahrampouri, M., Pajaro Miranda, C., Bradley, B. A., Nweke, C. C., Brandenberg, S. J., Donahue, J. L., Bozorgnia, Y., & Stewart, J. P. (2025a). Regional datasets included in the NGA-West3 ground motion database. *Geo-Extreme 2025*, in press.

Buckreis, TE, CC Nweke, P Wang, SJ Brandenberg, ME Ramos-Sepulveda, R Shams, S Mohammed, R Pretell, S Mazzoni, P Zimmaro, JP Stewart (2025b). A global application programming interface-enabled earthquake ground motion relational database for engineering applications, *Earthquake Spectra*, https://doi.org/10.1177/87552930251344978.

Buckreis, TE and JP Stewart, editors (2025c). Data resources for NGA-West3 project, PI: Yousef Bozorgnia, *Report GIRS-2025-07,* B. John Garrick Risk Institute, Natural Hazards Risk and Resiliency Research Center, UCLA (Center Headquarters), 418 pages.

Cakir, E., & Cetin, K. O. (2024). Liquefaction triggering and induced ground deformations at a metallurgical facility in Dörtyol-Hatay after the February 6 Kahramanmaraş earthquake sequence. *Soil Dynamics and Earthquake Engineering*, 178, 108465. https://doi.org/10.1016/j.soildyn.2024.108465

Cetin KO, Bray JD, Frost JD, Hortacsu A, Miranda E, Moss RES, Stewart JP (2023) February 6, 2023, Türkiye Earthquakes: report on geoscience and engineering impacts. Geotechnical Extreme Event Reconnaissance Association (GEER), the Earthquake Engineering Research Institute, and the Earthquake Engineering Foundation of Türkiye. *GEER Report 082*. https:// doi. org/ 10. 18118/G6PM34

Cetin, K. O., Ayhan, B. U., Cüceoğlu, F., & Yildirim, S. (2025). Performance of Reyhanlı Dam during February 6, 2023 Kahramanmaraş-Türkiye earthquake sequence. *Soil Dynamics and Earthquake Engineering*, 194, 109369. https://doi.org/10.1016/j.soildyn.2025.109369

Cetin, K. O., Cakir, E., Eyigün, Y., & Gokceoglu, C. (2024c). Soil liquefaction manifestations at Hatay Airport after the February 2023 Türkiye earthquake sequence. *Earthquake Spectra*, 41(1), 290-321. https://doi.org/10.1177/87552930241285024

Cetin, K. O., Cuceoglu, F., Ayhan, B. U., Yildirim, S., Aydin, S., Demirdogen, S., Er, Y., Gurbuz, A., & Moss, R. E. S. (2024a). Performance of hydraulic structures during 6 February 2023 Kahramanmaraş, Türkiye, earthquake sequence. *Earthquake Spectra*, 40(4), 2231–2267. https://doi.org/10.1177/87552930241258295

Çetin, K. Ö., Elsaid, A., & Ozacar, A. (2024d). Intensity characteristics of seismograms recorded during the February 6, 2023, M7.8 Türkiye Kahramanmaraş Pazarcik earthquake. Turkish *Journal of Civil Engineering*, 36(2), 29-51. https://doi.org/10.18400/tjce.1348206

Cetin, K. O., Moug, D., Soylemez, B., Ayhan, B. U., Zarzour, M., Suhaily, A. A., Akil, B., Unutmaz, B., Firat, S., Tekin, E., Cakir, E., Frost, D., Macedo, J., Bray, J., Moss, R., Bassal, P., Gurbuz, A., Işık, N. S., Akin, M., Sahin, A., Duman, E. (2024b). Ground failures and foundation performances in Adıyaman–Gölbaşı following the 6 February 2023 Kahramanmaraş–Türkiye Earthquake Sequence. *Earthquake Spectra*, 41(1), 249-289. https://doi.org/10.1177/87552930241270581

Dai, Z., Li, X., & Hou, C. (2013). A Shear-Wave velocity model for VS30 estimation based on a conditional independence property. *Bulletin of the Seismological Society of America*, 103(6), 3354–3361. https://doi.org/10.1785/0120130025

Elsaid, A., & Cetin, K. O. (2024). Duration Characteristics of Strong Ground Motions Recorded during the 6 February 2023 M 7.8 Pazarcık, Kahramanmaraş, Türkiye, Earthquake. *Seismological Research Letters*, 95(2A), 720–729. https://doi.org/10.1785/0220230300

Hudson, K.S., Ulmer K. J., Brandenberg S. J. (2024). Next Generation Liquefaction Software Tools, ngl_tools (Version 0.0.2) [Computer software]. DOI: 10.5281/zenodo.14004847

Karakas, V. E., Yildiz, I., Can, R., Kocaman, S., Cetin, K. O., & Gokceoglu, C. (2024). Event-based regional model of liquefaction susceptibility in Amik, Gölbaşı and Kahramanmaraş Basins after the February 6, 2023 Earthquakes. *Engineering Geology*, 339, 107644. https://doi.org/10.1016/j.enggeo.2024.107644

Kwak, DY, TD Ancheta, D Mitra, SK Ahdi, P Zimmaro, GA Parker, SJ Brandenberg, and JP Stewart (2017). Performance evaluation of VSZ-to-VS30 correlation methods using global VS profile database," *Proc. 3rd Int. Conf. on Performance-Based Design in Earthquake Geotechnical Engineering,,* M Taiebat, D Wijewickreme, A Athanasopoulos-Zekkos, and RW Boulanger (editors), Paper No. 399, Vancouver, BC.

Lashgari, A., & Moss, R. E. S. (2024). Displacement and damage analysis of earth dams during the 2023 Turkiye earthquake sequence. *Earthquake Spectra*, 40(2), 939-976.

Macedo, J., J. Bray, D. Moug, P. Bassal, C. Arnold (2025a). "Subsurface Characterization of Golbasi - 2023", in Subsurface Characterization of Selected Liquefaction Case Histories - 2023 Kahramanmaras Earthquake Sequence [Version 2]. DesignSafe-CI. https://doi.org/10.17603/ds2-frkc-z033

Macedo, J., J. Bray, D. Moug, P. Bassal, C. Arnold (2025b). "Subsurface Characterization of Iskenderun - 2024", in Subsurface Characterization of Selected Liquefaction Case Histories - 2023 Kahramanmaras Earthquake Sequence [Version 2]. DesignSafe-CI.

Moss, R. A., Seed, R. B., Kayen, R. E., Stewart, J., Kiureghian, A. D., & Cetin, K. (2006). CPT-Based Probabilistic and Deterministic Assessment of In Situ Seismic Soil Liquefaction Potential. *Journal of Geotechnical and Geoenvironmental Engineering*, 132(8), 1032–1051. https://doi.org/10.1061/(asce)1090-0241(2006)132:8(1032)

Moug D, Bassal P, Bray JB, Cetin KO, Kendir SB, Şahin A, Çakır E, Söylemez B, and Ocak S (2023) February 6, 2023, Türkiye Earthquakes: GEER Phase 3 team report on selected geotechnical engineering effects. Geotechnical Extreme Event Reconnaissance Association, *GEER Report 082-S1*.https:// doi. org/ 10. 18118/ G6F379

Moug, D., J. Bray, P. Bassal, S. Kendir, A. Sahin (2024a). "Lidar Scans of Geotechnical Earthquake Damage at Building Sites in Gölbaşı, Adıyaman", in GEER Lidar Data from the 2023 Kahramanmaras Earthquake Sequence Reconnaissance [Version 2]. DesignSafe-CI. https://doi.org/10.17603/ds2-fcry-0191

Moug, D., J. Bray, P. Bassal, A. Sahin, S. Kendir (2024b). "Lidar Scans of Liquefaction-Impacted Buildings in İskenderun, Hatay", in GEER Lidar Data from the 2023 Kahramanmaras Earthquake Sequence Reconnaissance [Version 2]. DesignSafe-CI. https://doi.org/10.17603/ds2-q5x1-e497

Moug, D. M., Bray, J. D., Bassal, P., Macedo, J., Ulmer, K., Cetin, K. Ö., Kendır, S. B., Şahin, A., Arnold, C., & Bikçe, M. (2024c). Liquefaction-induced ground and building interactions in İskenderun from the 2023 Kahramanmaraş earthquake sequence. *Earthquake Spectra*, 40(2), 913–938. https://doi.org/10.1177/87552930241232994

Ocak, S., & Cetin, K. O. (2024). Liquefaction-Induced failure of Demirköprü Bridge pile foundation and retaining system following the February 6 Kahramanmaraş earthquake sequence. *Journal of Earthquake Engineering*, 1–15. https://doi.org/10.1080/13632469.2024.2390096

Ozener, P., Monkul, M. M., Bayat, E. E., Ari, A., & Cetin, K. O. (2024). Liquefaction and performance of foundation systems in Iskenderun during 2023 Kahramanmaras-Turkiye earthquake sequence. *Soil Dynamics and Earthquake Engineering*, 178, 108433. https://doi.org/10.1016/j.soildyn.2023.108433

Ozkaynak, M. I., & Cetin, K. O. (2024). The performance of Karasu Bridge following the February 6, 2023 Kahramanmaras-Turkiye earthquake sequence. *Engineering Geology*, 335, 107512. https://doi.org/10.1016/j.enggeo.2024.107512

Pretell, R., T. Buckreis, S. Brandenberg, J. Stewart (2024). Spatial correlation models for ground motion intensity measures of the 2023 Türkiye-Syria Earthquakes. DesignSafe-CI. https://doi.org/10.17603/ds2-27yr-5m86

RocScience (2025). CPT Data Interpretation Theory Manual. https://static.rocscience.cloud/assets/verification-and-theory/Settle3/Settle3-CPT-Theory-Manual.pdf

Sahin, A., & Cetin, K. O. (2024). Liquefaction at two petrochemical facilities during the February 6, 2023, Kahramanmaras-Turkiye earthquake sequence. *Engineering Geology*, 335, 107539. https://doi.org/10.1016/j.enggeo.2024.107539

Ulmer K.J., Zimmaro P., Brandenberg S.J., Stewart J.P., Hudson K.S., Stuedlein A.W., Jana A., Dadashiserej A., Kramer S.L., Cetin K.O., Can G., Ilgac M., Franke K.W., Moss R.E.S., Bartlett S.F., Hosseinali M., Dacayanan H., Kwak D.Y., Stamatakos J., Mukherjee J., Salman U., Ybarra S., Weaver T. (2023). Next-Generation Liquefaction Database, Version 2. Next-Generation Liquefaction Consortium. DOI: 10.21222/C23P70.

Ulmer, KJ, KS Hudson, SJ Brandenberg, P Zimmaro, R Pretell, B Carlton, SL Kramer, JP Stewart (2024). Next Generation Liquefaction models for susceptibility, triggering, and manifestation, Rev 1, *RIL-2024-13*, US Nuclear Regulatory Commission, Research Information Letter, Office of Nuclear Regulatory Research, 233 pages.

Zhou J., (2023) VS30 Data of Turkey AFAD Strong-Motion Network Stations and VS30 Map of Turkey and Adjacent Area Related to the Feb. 2023 Turkey Seismic Sequence - 10/02/2023. DOI: 10.13140/RG.2.2.24389.12007